Dehancement effect of Au on Au diffusivity in Pb(Au) alloys

W. K. Warburton

Division of Engineering and Applied Physics, Harvard University, Cambridge, Massachusetts 02138

(Received 24 July 1974)

The effect of Au concentration on Au diffusivity was measured in dilute Pb(Au) alloys between 137 and 238 °C, and unusually large, negative linear coefficients b_{21} were found. The Au diffusivity is thus describable by the diffusion parameters at infinite dilution: $D_{20} = (3.62 \pm 0.36) \times 10^{-3}$ cm^2/sec, $H_2 = 8.94 \pm 0.09$ kcal/mole and the enhancement coefficient: $b_{21} = -(0.0500 \pm 0.0092) \exp(9.04 \pm 0.17)$ kcal mole$^{-1}/RT$). The classic interstitial-substitutional equilibrium model, commonly used to describe the fast-diffusing systems, is incompatible with this linear dehancement result. Rather, an equilibrium between Au singlets and Au doublets is required and provides a good description of the observations. The energy parameters from this model are significantly different from the values necessary to describe the low-temperature high-concentration Au precipitation and residual-resistivity results, as taken from the literature. The simplest resolution of this discrepancy is found by postulating a second equilibrium with Au multiplets, of three or four atoms, to explain the latter results. The structural possibilities for such clusters are investigated in terms of an extension of Hägg's rule.

I. INTRODUCTION

A variety of experiments has amply demonstrated that the Pb(noble metal) alloys, and Pb(Au) in particular, are rather peculiar systems and their study has provided a rich source of insights toward the development of alloy theory. These experiments have been comprehensively reviewed by several authors[1-4] and only the direct predecessors of the present work will be briefly mentioned here. Particularly, Au exhibits ultrafast diffusion in Pb, exceeding the self-diffusivity of Pb by factors of 10^6 to 10^4 between 100°C and the melting point of Pb at 327°C.[5-9] This behavior is intrinsic to the bulk alloy, being unaffected by the presence of grain boundaries[7] or of dislocations.[8] Further, the enhancement of Pb self-diffusion by Au is two orders of magnitude smaller than that required by a vacancy mechanism.[10] It is therefore generally agreed that the Au transport occurs primarily through the motion of some interstitial defect.[1]

More recently, Rossolimo and Turnbull (hereafter RT) indirectly measured Au diffusivity in Pb at low temperature by studying the kinetics of precipitation of $AuPb_3$ from Pb(Au) alloys.[11] The process was diffusion controlled, but the Au diffusivity was $2\frac{1}{2}$ to 4 orders of magnitude slower than predicted from an extrapolation of the high-temperature diffusivity. Figure 1 shows these results, labeled D_{plate} and D_{sphere}, which may be compared to the diffusivity of Au as extrapolated from high temperature (D_{Au}) and to the self-diffusivity of Pb (D_{Pb}). One of RT's tentative explanations for this effect was that diffusion-rate depression might result from a thermodynamic equilibrium between the rapidly diffusing Au interstitials and some second, less mobile, Au defect. If these second defects were energetically favored but entropically disfavored, as would be the case for pairs or small clusters of Au atoms, their fractional concentration would increase with decreasing temperature, producing the observed decrease in Au diffusivity.

RT also measured $\Delta\rho$, the residual resistivity per Au atom, in Pb, between −200 and 240°C for 0.0683- and 0.105-at.% alloys,[11] as shown in Fig. 2. The sharp increase in $\Delta\rho$ between 130 and 240°C, with some saturation near 240°C, is also explicable in terms of the two-defect equilibrium model stated above. Warburton[12] used a simple statistical thermodynamic calculation of defect concentrations to duplicate these resistivity curves theoretically, using appropriate defect resistivities and assuming one Au atom per defect in the high-temperature state and two Au atoms per defect in the low-temperature state (hereafter Au_1 and Au_2, respectively). The standard Gibbs-free-energy difference between defects giving the best fit to $\Delta\rho$ in the 0.0683-at.% Au alloy is

$$g^0_{2-1} = H^0_{2-1} - TS^0_{2-1}\,, \tag{1}$$

where

$$H^0_{2-1} = 9 \pm 2 \text{ kcal/mole}$$

and

$$S^0_{2-1} = 11.5 \pm 4.0 \text{ cal/mole °K}\,.$$

This corresponds to an absolute energy difference of 3.7 ± 2.7 kcal/mole at 185°C, in the middle of the transition region. Curves generated using (1) are superimposed on the data in Fig. 2. The

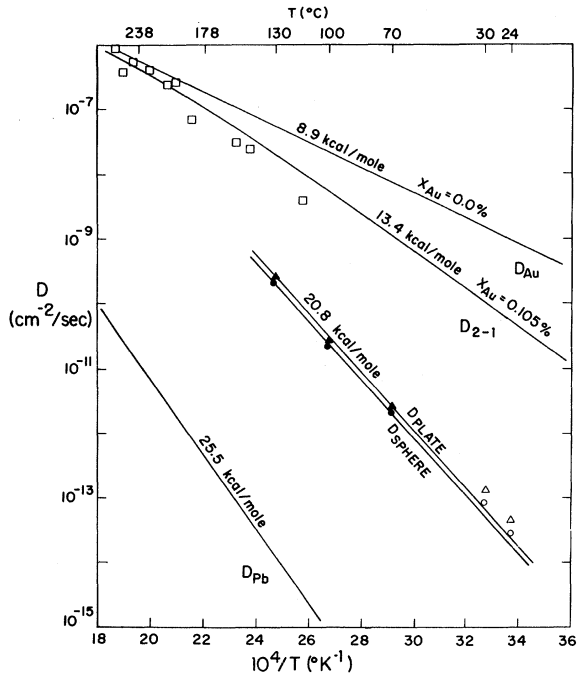

FIG. 1. Diffusivity of Au in Pb between 24 and 238°C, from several experiments. ▲, ● (△, ○) are from precipitation measurements of RT (Ref. 11) on a 0.105-(0.095-) at.% Pb(Au) alloy. □ are from Seith and Etzold (Ref. 6). The diffusivity of Au at infinite dilution, D_{Au}, is from this work, that at 0.105 at.%, D_{2-1}, is a calculation in the text. D_{Pb} is shown for comparison.

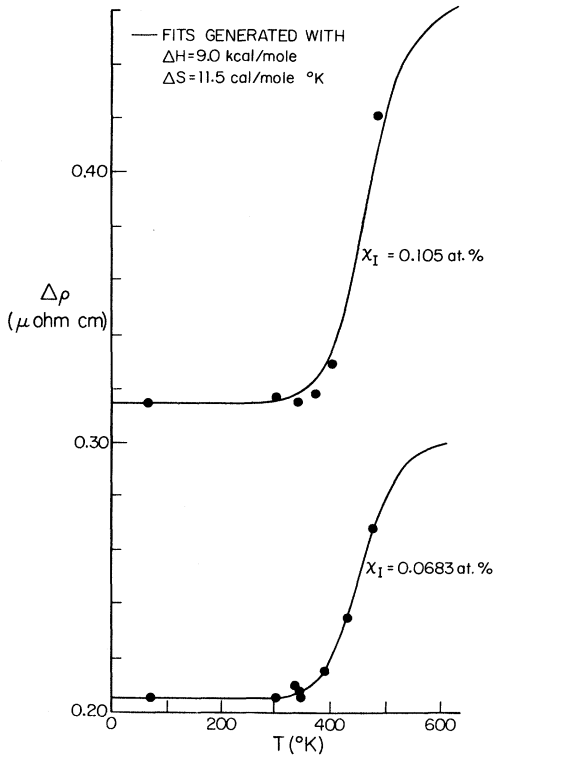

FIG. 2. Residual resistivity of Au in Pb as a function of temperature for two compositions. The fits were generated with a thermodynamic model using the indicated parameters.

major implication of this thermodynamic-equilibrium model to diffusion studies was that Au should dehance its own diffusivity in Pb, since increases in Au concentration would force the equilibrium toward an increased fraction of less-mobile Au_2 defects. The magnitude of the effect should vary inversely with temperature due to the $-TS$ term in (1) which favors the more mobile Au_1 defects.

Both these effects were observed in a series of exploratory measurements and found to be extremely large.[9] The present paper reports the results of a more careful study of this dehancement, including values between 138 and 238°C. The value of g^0_{2-1} consistent with the observed dehancements is extracted and found to be inconsistent with both Eq. (1), and the low-temperature diffusivity of Au in Pb found by RT. A simple resolution of this inconsistency is found by postulating the existence of a second equilibrium between Au_1's and higher-order Au clusters (Au_3 or Au_4). The structural possibilities for such defects are briefly explored in terms of an extension of Hägg's rule. Finally, the internal friction behavior[13-15] of Au in Pb is briefly examined in the light of these results.

II. EXPERIMENTAL DETAILS

The experiments were done on $\frac{1}{2}$-in.-diam single-crystal specimens grown by a modified Bridgman technique from Cominco 99.9999%-pure lead and commercial 99.999%-pure Au in Pyrex tubes backfilled to $\frac{1}{3}$ atm of He. Slugs 2 in. long were spark cut from the midsections of the resultant crystals, to avoid Au gradients in the ends, and annealed a week or more at from 215 to 250°C to remove any microsegregation. Since accurate analyses are difficult to obtain at these dilutions, alloy concentrations were assumed to be as compounded. Our experience with resistivity-measurement samples from different regions of the same slug indicates that the alloys are reasonably homogeneous. These slugs were spark cut to $\frac{1}{4}$-in. lengths to obtain the final samples. The following procedure, scrupulously followed, avoided surface holdup at all temperatures. Samples were waxed onto Al blocks with paraffin and microtomed 150 μm to remove spark-cutting damage, finishing with 2-μm cuts to leave a clean, min-

imally damaged surface. Sample sides and microtome blade were then dewaxed with trichloroethylene and acetone, a final 2-μm cut taken, the sample lowered to avoid surface damage by the blade's return stroke, and 0.2 ml of plating solution applied to the fresh face with a Schwarz-Mann biopette. The plating solution was made from 1-mCi ^{195}Au, supplied at 2 to 3 mCi/ml in 0.5N HCl by ICN Corp., and diluted with 6 ml of 0.5N HCL. Time from last cut to application of the plating solution was typically about 4 sec. The plating solution wet the clean face well and was confined to it by surface tension. Following a 1.5-min plate, the sample was inverted onto a cloth saturated with methanol and wiped to remove all traces of the plating solution. This step was particularly critical since even small amounts of the acid bath caused surface oxidation and resultant holdup. After a final wipe on a paper towel to remove the methanol, the sample was quickly warmed on a hotplate to dewax it from its block, cleaned of excess wax by a wipe on a trichloroethylene-soaked paper towel, wrapped in a small square of aluminum foil, and transferred to a Pyrex tube which was then evacuated. Time from the end of plating to evacuation was about 40 sec. All the samples for a given run were then sealed in a Pyrex tube at $\frac{1}{3}$ atm in He in order of increasing Au concentration.

Since the relative Au diffusivities in samples of different Au concentration vary by less than 20% before the solubility limit is reached at a given temperature, the samples at a given temperature must be annealed simultaneously and their thermal histories be made as identical as possible if an accurate measurement of the dehancement is desired. Therefore the tube containing the samples was immersed in a turbulently stirred bath of Dow Corning 210-H silicone fluid, which was heated resistively by a Bayley model-253 temperature controller. Bath temperatures were constant ± 0.05°C in the short term and ± 0.2°C overall for even the longest runs. Breakdown of the silicone fluid limited temperatures to less than 240°C. Because of the high stirring rate and thermal filtering through the Pyrex tube, differential temperatures between the samples are estimated to have been less than ± 0.01°C at all times after an initial 3-min upquench time, which was determined separately.

After the anneals the samples were rewaxed to their blocks with a stronger black wax with melting point about 130°C. The wax was melted on the blocks, the samples positioned, and the assemblies quenched on ice. Each sample was at elevated temperature less than 15 sec. The samples were then reduced in diameter on a lathe by at least 0.020 in. and sectioned. Sample diameters were measured after sectioning on an optical microscope fitted with a reticule and traveling stage, a technique which avoided inaccuracies due to deformation of the soft lead. The sections were weighed on a precision torsion balance with an accuracy of ± 0.02 mg. The increase in accuracy between the preliminary experiments and the present results is principally due to several stratagems which were adopted to enhance the accuracy of counting the activities of the sections. First, all sections were dissolved in 1 cm^3 of 65% acetic acid, 35% H_2O_2 solution, dispensed via metering syringe, in disposable polystyrene test tubes and covered with 1 cm^3 of Dow-Corning 200 silicone fluid at 10^5 centistoke to prevent splashing and ensure standardized geometry. Second, since the ^{195}Au's 0.129-MeV γ is slightly absorbed by the dissolved Pb, all sections were taken of the same thickness to eliminate variations due to this effect. Third, counting reproducibility was improved by reliably centering the test tubes in the standard scintillation vials required by the Picker Automatic β/γ counter used. This was done by winding a piece of $1\times3\times\frac{5}{16}$-in. low-density polyethylene foam, about 0.2 g/piece, into the bottom of each vial, leaving a hole which snugly accepted the test tubes. The foam did not noticeably attenuate counting rates. Fourth, in spite of the above precautions, random fluctuations in count rates due to locations of the vials in the counter occurred and it was necessary to count each set of sections 4 or 5 times to eliminate this effect. Counter windows were set from 0.110 to 0.150 MeV.

All diffusion profiles were strictly Gaussian, without serious holdup or noticeable non-Gaussian "tails" at maximum penetration. Individual points which deviated from the curves due to errors incurred in the weighing or dissolution processes were discarded before the data were fitted. Diffusion coefficients were extracted from the data in the usual manner as reported earlier.[16]

III. EXPERIMENTAL RESULTS

A representative set of diffusion-penetration profiles, obtained from alloys of between 0.0000 and 0.003-at.% Au at 138°C is shown in Fig. 3, plotting $\log_{10}$ (activity) versus penetration squared. The curves were strictly Gaussian, as were all the curves obtained once initial holdup difficulties were overcome. The values of activity shown in Fig. 3 span approximately 1.2 decades, which is slightly larger than the typical 0.9 to 1.0 decades. Although it is usual to measure activity over 2 or more decades in an unexplored system, the diffusion of Au in pure Pb is well studied and the

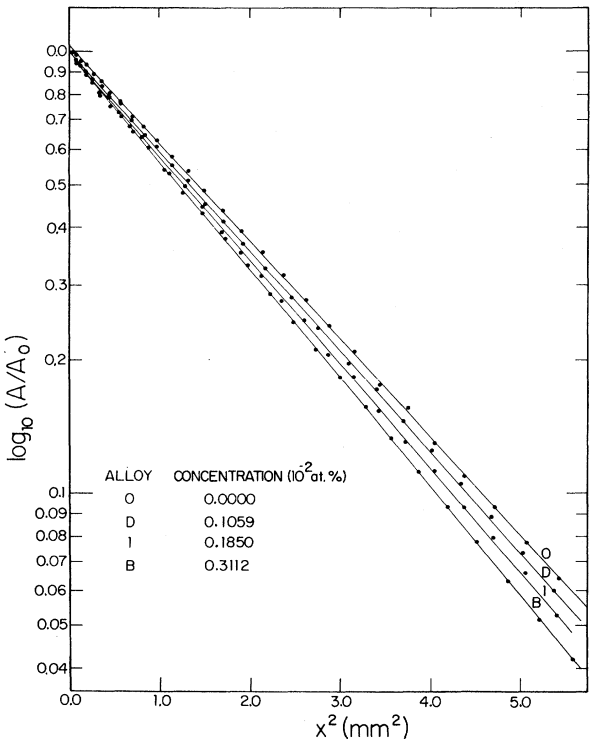

FIG. 3. Diffusion profiles in four samples of the indicated compositions at 137°C.

range of penetrations was restricted for several reasons. First, in order to determine slopes with sufficient accuracy, at least 10^4 counts are necessary for each section. Since there was also reason to believe that even the amount of Au in the tracer might affect its own diffusivity, it was deemed advisable to keep tracer activity as low as could be conveniently handled. Thus, with 10^4 counts per minute in the first section, sections more than a decade down in activity begin both to require excessive amounts of counter time and also to require more than a few percent correction for background, the constancy of which, in an environment of moving sources, may not be arbitrarily assumed.

We are quite confident, however, that even with the somewhat limited ranges of activity, the diffusivities obtained are indeed characteristic of bulk Au diffusivity in alloys of the indicated Au concentrations. First, the experiment at 158°C had activity decrements of over 1.6 decades and the penetration profiles were still Gaussian. Second, no systematic deviations from linearity were observed in any of the curves reported. Third, in those diffusion situations where penetration profiles are observed to be kinked, with two relatively straight sections, it is necessary to have at least one and usually several orders of magnitude difference in relative diffusivities in order for the individual sections to be relatively straight. Since the measured diffusivities are about 10^{-7} cm^2/sec, with penetrations of the order of 2 mm, it is extremely unlikely that this condition could be fulfilled.

TABLE I. Alloy compositions by atomic fraction, in parts per million.

Alloy	Au concentration	Alloy	Au concentration
0	0.00±0.01	*F*	99.58±0.28
1	18.50±0.20	*G*	150.82±0.32
2	38.2±0.25	*H*	301.43±0.43
4	100.1±0.35	*I*	402.38±0.49
A	5.63±0.17	*J*	499.95±0.49
B	31.12±0.17	*K*	599.04±0.56
C	59.46±0.16	*L*	199.83±0.33
D	10.59±0.20		

The diffusivities obtained at each temperature are listed in Table II (alloy compositions in Table I), and plotted for four temperatures: 238, 218, 158, and 138°C in Fig. 4. The maximum alloy concentration used at each temperature was set well below the Au solubility limit.[11] These four dehancement curves are typical, being fairly straight for diffusivity decrements up to about 12% (238 and 138°C) and showing some positive curvature for larger decrements (218 and 158°C). As can be seen from all these figures, there is still a certain amount of scatter in the data beyond what would be expected purely on grounds of statistical scatter, and the source of these deviations continues to elude us. That they exist is not in itself surprising when it is noted that the maximum decrement in diffusivity before the solubility limit is reached is about 25% and is more typically 10% at the lower temperatures.

The most interesting feature of these curves is the extreme magnitude of the dehancements involved. At 228°C at 27% decrease in diffusivity is produced by an addition of 0.06-at.% Au to the Pb and at 138°C a 10% decrease in diffusivity is produced by only 30-ppm Au impurity. The curves were fit by the standard expression:

$$D_2(x) = D_2(0)\,(1.0 + b_{21}x + b_{22}x^2 + \cdots)\,, \qquad (2)$$

where $D_2(0)$ is the diffusivity of Au in a pure Pb host, x is the Au concentration, and the b's are enhancement coefficients. In the present case only the linear term is reported. Least-squares fits were made to the data at all temperatures and the resultant values of $D_2(0)$ and b_{21} are presented in Table III. In particular, the values of $D_2(0)$

TABLE II. Diffusivities measured in Pb(Au) alloys for the different isothermal diffusion anneals. Alloy compositions are listed in Table I. Diffusivities are in 10^{-7} cm^2/sec, their standard errors in 10^{-9} cm^2/sec, temperatures in °C.

T	Alloy	D	σD	T	Alloy	D	σD
238.0±0.2	0	5.609	3.7	178.0±0.2	0	1.652	0.39
	F	5.496	5.1		*A*	1.640	0.48
	L	5.172	3.4		*D*	1.620	0.35
	H	4.789	1.8		1	1.600	0.50
	I	4.729	2.6		*B*	1.595	0.54
	J	4.650	3.2		2	1.573	0.54
	K	4.375	2.4		*C*	1.537	0.53
					4	1.460	0.45
228.2±0.1	0	4.581	2.2	166.5±0.2	0	1.283	0.38
	F	4.358	3.4		*A*	1.276	0.47
	L	4.243	2.0		*D*	1.274	0.78
	H	3.944	1.9		1	1.242	0.67
	I	3.753	1.6		*B*	1.229	0.50
	J	3.780	1.9		2	1.205	0.47
	K	3.365	2.4		*C*	1.172	0.36
					4	1.106	0.59
217.8±0.2	0	3.907	2.3	158.0±0.2	0	1.0410	0.21
	C	3.759	1.9		*A*	1.0339	0.20
	F	3.669	2.5		*D*	1.0189	0.28
	G	3.599	1.5		1	0.9992	0.22
	L	3.434	2.3		*B*	0.9798	0.22
	H	3.206	2.6		2	0.9572	0.29
	I	3.155	1.7		*C*	0.9394	0.10
	J	2.953	1.7				
	K	2.978	1.6				
205.7±0.2	0	2.048	1.7	149.0±0.5	0	0.8804	0.13
	B	3.052	2.2		*A*	0.8741	0.19
	C	2.898	1.8		*D*	0.8391	0.17
	F	2.828	2.0		*B*	0.8113	0.15
	G	2.735	1.7		2	0.7914	0.17
	L	2.656	1.5		*C*	0.7498	0.12
	H	2.458	1.2	145.0±0.2	0	0.7575	0.10
	I	2.372	1.0				
	J	2.240	0.8	137.3±0.2	0	0.6555	0.19
					D	0.6339	0.13
					1	0.6113	0.15
					B	0.5892	0.12

represent the best estimates of the diffusivity of Au in Pb at infinite dilution obtainable from the present data. The values of b_{21} are also immediately striking, in that they range from about -300 to -3000 when typical enhancement values in substitutional alloys[17] are in the range -10 to $+50$, and even these are not strictly comparable, being values of *solvent* enhancement by the impurity. Few values of *impurity* enhancement have been reported, with the exception of Cd and Hg in Pb,[16, 18] where the values were positive in the range $+20$ to $+30$, and Pb in Ag,[17] where b_{21} was approximately $+500$.

An Arrhenius plot of the values of $D_2(0)$ is shown in Fig. 5 and they may be seen to fall on a straight line over a full decade. The estimated error in the values of $D_2(0)$ is somewhat less than the size of the points on the figure. A least-squares fit gives the following values for the diffusion parameters for Au in pure Pb:

$$D_2^0 = (3.62 \pm 0.36) \times 10^{-3} \text{ cm}^2/\text{sec} ,$$
$$H_2 = 8.94 \pm 0.09 \text{ kcal/mole} . \quad (3)$$

No curvature was suggested by the individual deviations of the data points from the best-fit line. The values reported by Ascoli,[7] Kidson,[8] and Seith and Etzold[6] have been included on Fig. 5 and generally agree with the present work, especially at higher temperatures. The values of the dif-

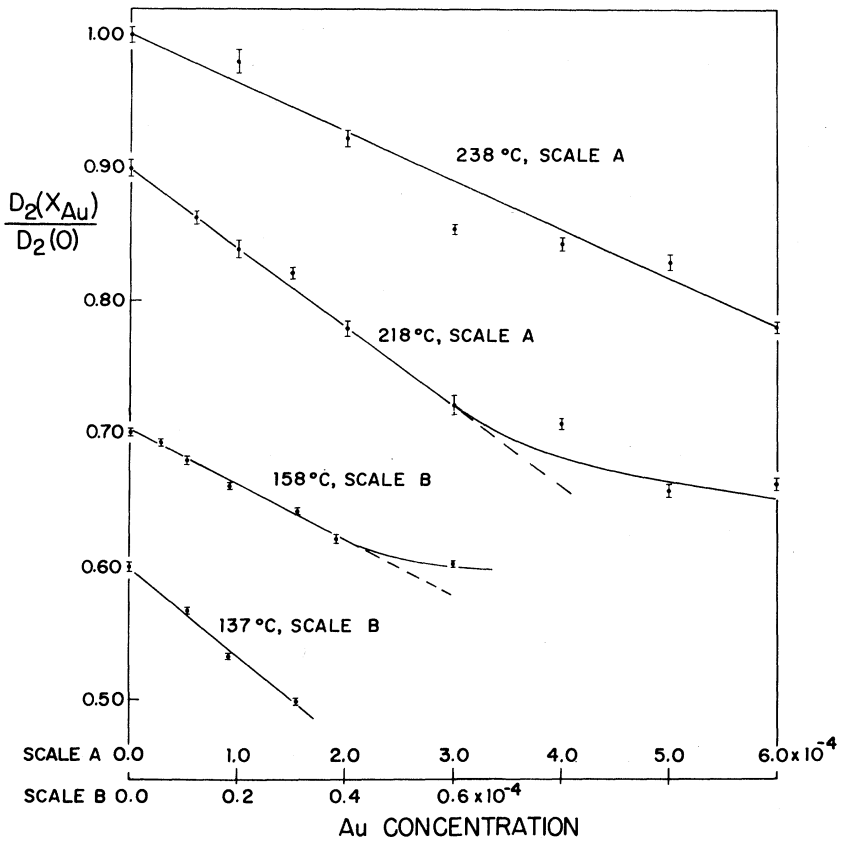

FIG. 4. Dehancement curves at 238, 218, 158, and 137°C; diffusivity versus alloy composition. The error bars represent standard errors obtained from the least-squares fits. The curves at 218, 158, and 137°C have been displaced for clarity.

fusion parameters extracted from the three sets of data may be compared in Table IV. On closer inspection, however, it appears that all of our values of $D_2(0)$ lie above those of the previous workers, excepting only Kidson's measurements using an extremely dilute ^{199}Au tracer. Correspondingly, our values of the heat of diffusion H_2 and preexponential D_2^0 are both smaller than those previously reported and their accuracy is sufficient for the differences to be significant. In view of the ability of Au to dehance its own diffusion, as established by this work, it seems reasonable to expect that these differences are most likely attributable to differences in the concentration of Au tracer used by the various investigators.

When an Arrhenius plot of the values of $-b_{21}$ is made, as shown in Fig. 6, it may be seen that they too fall on an essentially straight line. The least-squares fit to the data give preexponential and energy values of

$$-b_{21}^0 = 0.0500 \pm 0.0092 \ , \qquad H_b = 9.04 \pm 0.17 \text{ kcal/mole} \ . \tag{4}$$

The significance of this result will be examined in detail in Sec. V A.

IV. THEORETICAL EQUILIBRIUM CONSIDERATIONS

It seems clear, for the reasons cited in the Introduction, that some sort of interstitial defect is responsible for the diffusion behavior of Au in Pb at high temperatures and low concentrations. However, it is also evident that no single defect of any type can account for the full range of behavior observed in this system. Therefore, if we assume that several defect states are allowed for Au in Pb and that we are usually examining our

TABLE III. Values of $D_2(0)$ and b_{21} as a function of temperature. $t^2 = \chi^2/(n-2)$ and measures the goodness of fit.

T (°C)	Alloys omitted	t^2	$D_2(0)$ (10^{-7} cm^2/sec)	b_{21}
238.0±0.2	H	3.1	5.609±0.041	−367±41
228.2±0.1	L, J	3.6	4.569±0.010	−444±7
217.8±0.2	I, J, K	1.7	3.910±0.022	−582±34
205.6±0.2	I, J	2.9	3.045±0.018	−646±32
178.0±0.2		2.3	1.646±0.0048	−1130±46
166.5±0.2	4	1.1	1.284±0.0031	−1490±65
158.0±0.2	C	2.2	1.042±0.0026	−1990±106
149.0±0.5	D	4.0	0.8813±0.0021	−2540±64
137.3±0.2		4.3	0.6551±0.0026	−3290±210

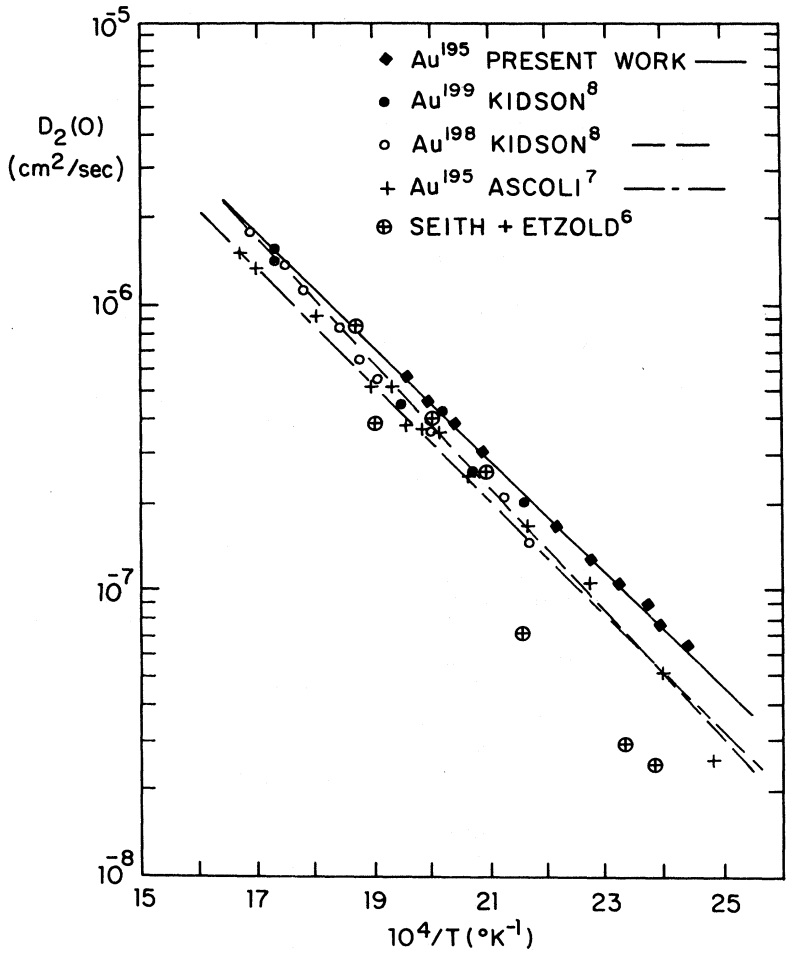

FIG. 5. Diffusivities of Au in Pb at nominally infinite dilution as a function of temperature. The results of the present work are compared to those of earlier studies.

systems under equilibrium conditions, or nearly so, then it is reasonable to explore statistical thermodynamic arguments concerning the dependence of defect concentrations on temperature and total impurity concentration. This is done in Sec. IV A. In Secs. IV B and IV C, the equilibria $Au_1^{\alpha} \rightleftharpoons Au_1^{\beta}$ and $2Au_1 \rightleftharpoons Au_2$ are specifically examined. The notation Au_N refers to a defect having N Au atoms and will be called a singlet, doublet, N-tuplet, etc.

A. Statistical thermodynamics of defect equilibrium

It follows from general statistical thermodynamic arguments[12] that if N defect species are in equilibrium in an alloy where the total impurity concentration x_I is small, as they are in the present system where $x_I \leq 0.06$ atom fraction, then the atom fraction of the kth defect, x_k, is given by

$$x_k = \frac{\rho_k}{\rho_N^{\delta_k}} e^{-g_{N-k}^0/RT}\left(\frac{x_I}{d_N} + \sum_{i=1}^{N-1} \psi_i x_i\right)^{\delta_k} . \qquad (5)$$

Here g_{N-k}^0 is the usual chemical notation for standard Gibbs free-energy change per mole of Au on going from state N to state k. ρ_k is the number of distinct orientations the kth defect can have about its assigned lattice site, d_k is the number of Au atoms per type-k defect, and $\delta_k = d_k/d_N$. Now ψ_i is given by $\psi_i = -(\delta_i + C_I\beta_i)$ where, since δ_i and β_i are of order unity and $C_I \approx x_I/d_N$, we have $\psi_i \approx -\delta_i$ in the present limit of very dilute alloys.

TABLE IV. Diffusion parameters obtained for Au in Pb by various workers.

D_{Au}^0 (cm^2/sec)	H_D (kcal/mole)	Study	Date	Ref.
0.35	14.0	Seith and Etzold	1934	6
4.1×10^{-3}	9.35 ± 0.07	Ascoli	1960	7
8.7×10^{-3}	10.0	Kidson	1966	8
$(3.62\pm0.36)\times10^{-3}$	8.94 ± 0.09	this study	1975	

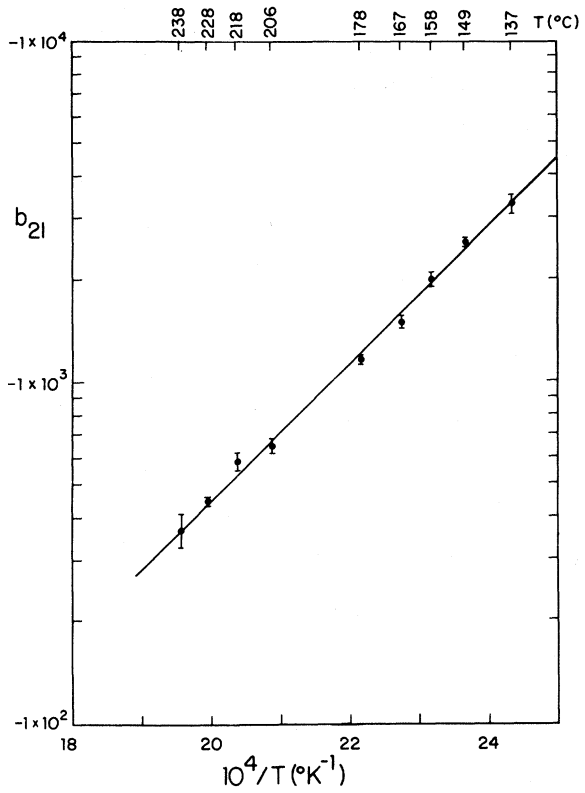

FIG. 6. Dehancement coefficients b_{21} as a function of temperature. Plotted is $\log_{10}(-b_{21})$ vs $1/T$.

Thus writing $a_k = \rho_k/(d_N\rho_N)^{\delta_k}$, we have

$$x_k = a_k\, e^{-g^0_{N-k}/RT}\left(x_I - \sum_{i=1}^{N-1} d_i\, x_i\right)^{\delta_k} , \tag{6}$$

and, to conserve Au atoms,

$$x_I = \sum_{i=1}^{N} d_i\, x_i \ . \tag{7}$$

Thus, in more physical terms, a_k results from changes in orientational configurational entropy on going from an N defect to a k defect. The bracketed term in Eq. (6), from Eq. (7), is just $d_N x_N$, the number of Au atoms in the type-N defect state, and the quantity $(d_N x_N)^{\delta_k}$ results from changes in positional configurational entropy on going from an N defect to a k defect. Vibrational entropy changes are found, by definition, in g^0_{N-k}. δ_k is the number of N defects required to form a single k defect. Notice that in the foregoing the standard thermodynamic state, from which all energy differences are measured, is the alloy with all defects in the N state.

Now our stated goal is to discover models in which dehancement can occur. To produce concentration effects, such models will clearly require Au defect species having different diffusivities. Considering this simplest possibility and labeling the fast diffusing defect 1 and the slower defect 2, Eqs. (6) and (7) become

$$x_1 = a_1\, e^{-g^0_{2-1}/RT}(x_I - d_1 x_1)^{\delta_1} \tag{8}$$

and

$$x_I = d_1 x_1 + d_2 x_2 \ . \tag{9}$$

The diffusivity of Au in this system will be

$$D_{\mathrm{Au}} = D_1\,\frac{d_1 x_1}{x_I} + D_2\,\frac{d_2 x_2}{x_I} , \tag{10}$$

which, by application of Eq. (9), becomes

$$D_{\mathrm{Au}} = \frac{d_1 x_1}{x_I}\,(D_1 - D_2) + D_2 , \tag{11}$$

where, by definition, $(D_1 - D_2)$ is positive. For a given system, Eq. (8) may be solved for x_1, which, substituted into Eq. (10), describes the system diffusion behavior as a function of x_I and T. These results are subject only to the assumptions of low concentrations and of only two defect types. We next deduce the general behavior of this system by considering the two limits: g^0_{2-1} large and positive and g^0_{2-1} large and negative.

Case 1: g^0_{2-1} large and positive, $d_1 x_1 \ll x_I$. Under these conditions we may neglect $d_1 x_1$ with respect to x_I in Eq. (8) and solve directly for x_1 to obtain

$$D_{\mathrm{Au}} = D_2 + (D_1 - D_2)\, a_1\, e^{-g^0_{2-1}/RT}\, x_I^{\delta_1 - 1} . \tag{12}$$

The value of b_{21} may be found from the slope of D_{Au} vs x_I as x_I goes to zero if $\delta_1 \neq 1$:

$$b_{21} = \frac{D_1 - D_2}{D_2}\,(\delta_1 - 1)\, a_1\, e^{-g^0_{2-1}/RT}\, x_I^{\delta_1 - 2} . \tag{13}$$

A linear enhancement corresponds to the value $\delta_1 = 2$, so that b_{21} is strictly positive. No dehancements are possible. Except for fractional δ_1 values, in which case the effect diverges as $x_I \to 0$, this case corresponds to the classic case of impurity self-enhancement in substitutional alloys. If we further restrict ourselves to observing values of b_{21} in the high-temperature limit, then, writing $g^0_{2-1} = H^0_{2-1} - TS^0_{2-1}$, we must have $S^0_{2-1} < 0$ for g^0_{2-1} to be large and positive for large T and two subcases are possible as H^0_{2-1} may either be positive or negative. In the former case ($H^0_{2-1} > 0$, $S^0_{2-1} < 0$), from Eq. (13), $|b_{21}|$ will increase with increasing temperature, while in the latter case ($H^0_{2-1} < 0$, $S^0_{2-1} < 0$) $|b_{21}|$ will decrease with increasing temperature.

Case 2: g^0_{2-1} large and negative, $d_1 x_1 \approx x_I$. Under these conditions we approximate x_1 by x_I/d_1 on the left of Eq. (8) and solve for $\Delta = x_I - d_1 x_1$. Then, writing x_1 in terms of Δ and substituting into Eq.

(11), we obtain

$$D_{\mathrm{Au}} = D_1 - (D_1 - D_2)\left(\frac{1}{a_1 d_1}\, e^{g^0_{2-1}/RT}\right)^{1/\delta_1} x_I^{1/\delta_1 - 1} . \tag{14}$$

Similarly to case 1, we find b_{21} from the slope of D_{Au} as $x_I \to 0$, assuming $\delta_1 \neq 1$:

$$b_{21} = -\frac{D_1 - D_2}{D_1}\left(\frac{1}{a_1 d_1}\, e^{g^0_{2-1}/RT}\right)^{1/\delta_1}\left(\frac{1}{\delta_1} - 1\right) x_I^{1/\delta_1 - 2} . \tag{15}$$

Equation (15) is important since it shows the possibility of dehancements resulting for values of the defect-impurity atom ratio δ_1 such that $0 < \delta_1 \leq \frac{1}{2}$. In particular, the case of a linear dehancement corresponds to $\delta_1 = \frac{1}{2}$, which is associated with an equilibrium between Au_1 and Au_2 defects, the *former* being more stable at the temperature of interest. For the more general equilibrium between Au_1 and Au_n defects, we see from Eq. (14) that the diffusivity behaves as x_I^{n-1} as $x_I \to 0$. The general case of Au_m equilibrium with Au_n is obvious from Eq. (14) and will not be discussed. Proceeding as in case 1, we require $S^0_{2-1} > 0$ for g^0_{2-1} to be large and negative at high-T values, and the two subcases are ($H^0_{2-1} > 0$, $S^0_{2-1} > 0$), which gives $|b_{21}|$ decreasing with increasing T, and ($H^0_{2-1} < 0$, $S^0_{2-1} > 0$), which gives $|b_{21}|$ increasing with increasing temperature.

B. Equilibrium $\mathrm{Au}_1^{\alpha} \leftrightarrow \mathrm{Au}_1^{\beta}$

This class of singlet-singlet equilibria includes the classic dissociative diffusion mechanism[2,19] which results from the equilibrium between monatomic substitutionals and interstitials as well as the more recently proposed equilibrium between interstitial-vacancy pairs and monatomic substitutionals.[3,10] The important result for this class of equilibria, for which $\delta_1 = 1$, is that D_{Au} is independent of x_I, as may be seen from Eqs. (12) and (14) in the two limiting cases. This result is in fact independent of the value of g^0_{2-1}, as may be easily seen by solving Eq. (8) directly for x_1, which will be linear in x_I, and substituting into Eq. (11) for D_{Au}, where x_I cancels out. We therefore conclude that the dissociative diffusion mechanism in particular and equilibria between defects with equal numbers of Au atoms in general are unable to explain the presently observed dehancement of Au diffusion.

C. Equilibrium $2\mathrm{Au}_1 \leftrightarrow \mathrm{Au}_2$

For the case of singlet-doublet equilibrium, Eq. (6) becomes

$$x_1 = \alpha_1 (x_I - x_1)^{1/2} , \tag{16}$$

where α_1 is $a_1 e^{-g^0_{2-1}/RT}$ The solution for x_1 is found from the quadratic equation and substituted into Eq. (11) to give

$$D_{\mathrm{Au}} = D_2 + (D_1 - D_2)\,\frac{\alpha_1^2}{2x_I}\left[\left(1 + \frac{4x_I}{\alpha_1^2}\right)^{1/2} - 1\right] , \tag{17}$$

which may be expanded in the limit of small impurity concentration x_I to give

$$D_{\mathrm{Au}} = D_2 + (D_1 - D_2)\left(1 - \frac{x_I}{\alpha_1^2} + \frac{2x_I^2}{\alpha_1^4} - \frac{5x_I^3}{\alpha_1^6} + \cdots\right) , \tag{18}$$

showing the specific relationship between α_1^2 and b_{21}, the linear impurity enhancement coefficient, to be

$$b_{21} = -\alpha_1^{-2} . \tag{19}$$

Further, an examination of Eq. (17) shows that all the temperature dependence resulting from the equilibrium resides in α_1, and may be removed via the scaled variable $c = 4x_I/\alpha_1^2$, to give

$$D_{\mathrm{Au}} = D_2 + (D_1 - D_2)\,(2/c)\left[(1+c)^{1/2} - 1\right] . \tag{20}$$

The initial slope of D_{Au} versus c is $-1/4(D_1 - D_2)$, by comparison to Eq. (18).

V. INTERPRETATION

A. Dehancement data

It follows from Eqs. (14) and (15) that a singlet-doublet equilibrium of the type described is a necessary and sufficient condition for the production of a linear diffusivity dehancement. The linearity of $\ln(-b_{21})$ vs $1/T$, as described by the coefficients of Eq. (4), is then in agreement with the predictions of Eq. (19), which becomes

$$-b_{21} = \rho_1 (2\rho_2)^{-1/2}\, e^{2g^0_{2-1}/RT} . \tag{21}$$

Values of H^0_{2-1} and S^0_{2-1} may then be extracted from Eq. (4) by the use of Eq. (21) if values are assigned to the model-dependent ρ's, the defect orientation factors. This was done for two doublet models, taken from the literature[1,11] and listed in Table V. The resultant values of H^0_{2-1} and S^0_{2-1} seem reasonable by comparison to the corresponding values for vacancy formation, for which Leadbetter *et al.*[20] found $H_v = 13.4 \pm 3.0$ kcal/mole and Feder and Nowick[21] found $H_v = 11.3 \pm 2.3$ kcal/mole and $S_v = 1.4 \pm 4.0$ cal/mole °K.

An estimate of the doublet diffusivity was attempted by fitting the data at each temperature to the full form of Eq. (17). Values of D_2 were obtained which were less than $\frac{1}{10}$ the magnitude of D_1 and scattered equally between positive and negative values. Thus, to experimental accuracy, $D_2 \approx 0$, when compared to D_1, which is hardly sur-

TABLE V. Standard Gibbs free-energy difference per Au atom between the Au singlet state and the various other Au defect or precipitation states.

Second state	Enthalpy (kcal/mole)	Entropy (cal/mole °K)	Source
doublet (i_2-V triplet)	4.52 ± 0.08	$1.20^{+0.21}_{-0.16}$	b_{21} vs T
doublet (Au-Au dimer)	4.52 ± 0.08	$2.82^{+0.21}_{-0.14}$	b_{21} vs T
triplet	11.9	13.3–13.6	Diffusivity during precipitation
quadrupet	11.9	6.7	Diffusivity during precipitation
$AuPb_3$	16.9	21.3	Au solubility

prising, considering that some coordinated mechanism would be required for doublet diffusion.

A final test was made of the applicability of the singlet-doublet equilibrium model to the present system by making a plot of diffusivity versus reduced concentration of the sort suggested by Eq. (20). If D_2 is negligible compared to D_1, we have

$$D_{Au}/D_1 = 2c^{-1}[(1+c)^{1/2} - 1] , \qquad (22)$$

which has been plotted in Fig. 7 together with the experimental diffusivity ratios. As required by Eq. (19), the experimentally determined b_{21} values were used to scale the concentrations. Figure 7 reveals the curious fact that, while experiment and theory agree up to values of $c \approx 0.2$, the experimental points for values of $c \lesssim 0.6$ continue to fall on a straight line of slope $-\frac{1}{4}$, the value predicted by Eq. (22) as $c \to 0$. Beyond $c \approx 0.6$, the data points begin to deviate in the expected direction, but never so much as predicted.

The experimental situation, then, is that dehancements occur which are in *excess* of the amounts predicted by a simple singlet-doublet (SD) defect equilibrium model. This situation is not relieved by postulating the presence of another singlet-type defect, as for example in the equilibria substitutional ⇌ doublet ⇌ interstitial (SDI) or doublet ⇌ interstitial-vacancy pair ⇌ interstitial (DPI). This may be shown by a simple calculation beginning with Eq. (6) or intuitively understood by recalling that a singlet-singlet equilibrium shows no dehancement and realizing that the three defect cases will show behavior intermediate between the limiting cases in which the concentration of either the doublet or of one of the singlets becomes zero. Thus both SDI and DPI dehancements are smaller than in the pure-SD case, which implies that Au substitutionals do not occur to any appreciable extent in Pb.

A singlet ⇌ doublet ⇌ multiplet equilibrium (SDM), on the other hand, is capable of producing excessive dehancements. This may be seen by considering the high-temperature limit where all the impurity is essentially in the singlet state. The doublet and multiplet concentrations are essentially independent of each other and result in additive decreases in D_{Au} proportional respectively to x_I and x_I^{m-1} [Eq. (14)]. An SDM equilibrium will therefore produce larger dehancements than a simple SD equilibrium, as observed. Section V B shows that the assumption of a multiple-defect equilibrium will also resolve discrepancies between the present work and that of RT.

B. Residual resistivity and Au precipitation results of RT

A comparison of the values of H^0_{2-1} and S^0_{2-1} obtained from the dehancement work (Table V) and from RT's Au residual-resistivity work [Eq. (1)] shows them to be in sharp disagreement. The enthalpies differ by a factor of 2 and the entropies by a factor of at least 5, depending on the doublet model chosen. The values from the dehancement work are also incapable of describing the low-temperature Au diffusivity found in RT's precipitation studies. This is shown in Fig. 1, where $D_{Au}(T, X)$ has been determined from Eq. (17) for an 0.105-at.% alloy, and plotted as D_{2-1}. These $D_{Au}(T, 0.105)$ values lie substantially below the high-temperature extrapolation of $D_{Au}(T, 0)$ but are several order of magnitude above the precipitation results. Further, they show an incorrect value of low-temperature limiting slope, about 13.4 kcal/mole instead of the observed 20.8 ± 0.6 kcal/mole. Finally, they cannot even reproduce the low-temperature Seith and Etzold[6] results,

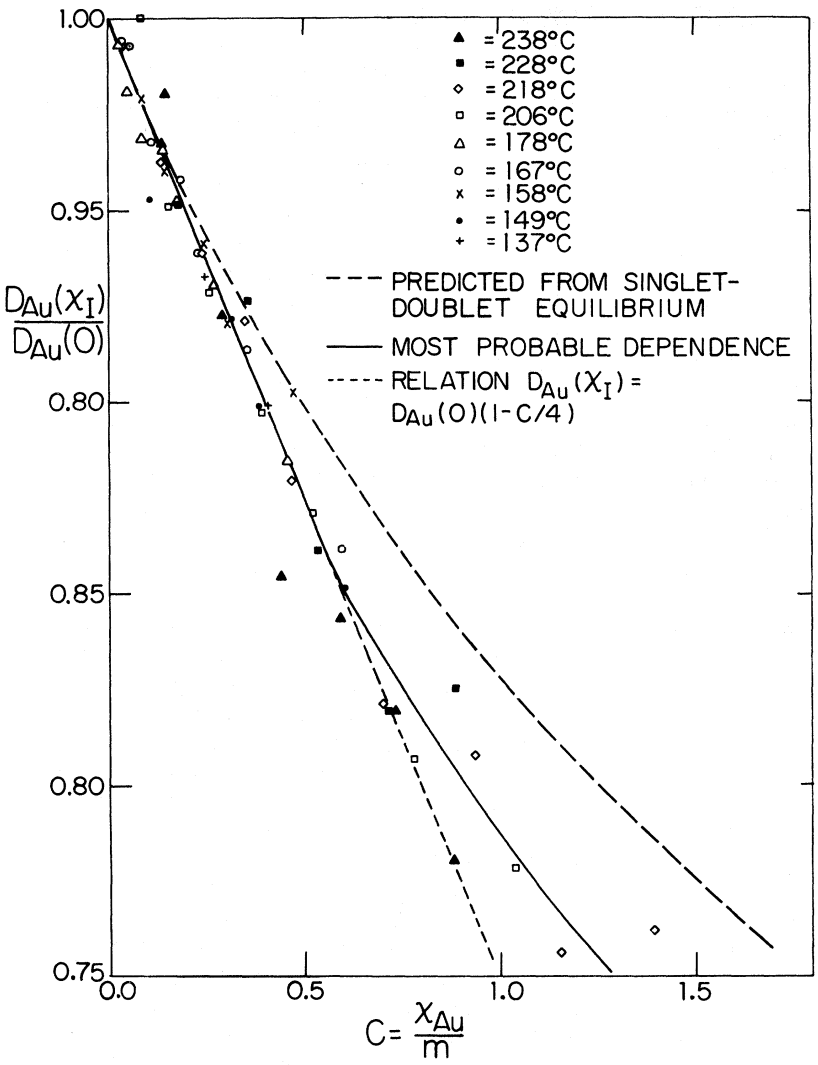

FIG. 7. Dehancement data versus scaled concentration. The temperature dependence has been removed by the scaling term $m=\delta_1^2/4 = -1/4b_{21}$ [Eqs. (19) and (20)].

which are definitely equilibrium measurements and at far lower concentration values.

The precipitation result is describable by a singlet–N-tuplet equilibrium model, for $N \geq 2$, provided the proper values of H^0_{N-1} and S^0_{N-1} are chosen. We are now in the low-temperature high-concentration regime where most of the Au is in N-tuplets. This corresponds to case 1 of Sec. IV A and, assuming $D_2 = 0$ for simplicity, Eq. (12) becomes

$$D_{Au}(T, x_I) = D_1 a_1 x_I^{1/N-1} e^{-g^0_{N-1}/RT} \qquad (23)$$

where D_1, the Au-singlet diffusivity, is given by $D_1^0 e^{-H_2/RT}$. An Arrhenius plot of $D_{Au}(T, x_I)$ vs $1/T$ in this region will thus shown an effective activation enthalpy of diffusion of $H' = H_2 + H^0_{N-1}$, where we recall $g^0_{N-1} = H^0_{N-1} - TS^0_{N-1}$. Thus, subtracting the observed value of $H_2 = 8.9 \pm 0.1$ kcal/mole [Eq. (3)] from the value 20.8 ± 0.6 given above, we obtain $H^0_{N-1} = 11.9 \pm 0.7$ kcal/mole, in remarkable agreement with the value in Eq. (1), 9 ± 2 kcal/mole. We may therefore conclude that the precipitation and residual-resistivity results are consistent with each other and mutually inconsistent with the dehancement results.

This inconsistency is readily removed, as suggested in Sec. V A, by postulating the formation of a higher-order Au defect. The values of g^0_{N-1} obtained from the precipitation and residual-resistivity studies would now describe a different equilibrium and not be expected to equal the values of g^0_{2-1} obtained from the dehancement work. The most likely defect might be an Au triplet, since this could most easily be used to explain the excessive linearity of Fig. 7. Quartets, however, might also be a possibility.

C. Defect standard free energies

The standard free-energy differences between Au singlets and Au doublets was calculated in Sec. V A and listed in Table V. Similarly, values for g^0_{N-1} may be calculated from Eq. (12), using RT's value for $D_{Au}(T, 0.105)$ for $x_I = 0.105$-at.% Au:

$$D_{Au}(T, 0.105) = (45\ \mathrm{cm^2 sec^{-1}})\, e^{-20.8\ \mathrm{kcal\ mole^{-1}}/RT}, \tag{24}$$

assuming $D_2 = 0$ and making reasonable estimates of a_1. These values are also listed in Table V. Finally, from the equilibrium solubility of Au at high temperatures ($AuPb_3 \rightleftharpoons Au_1 + 3Pb$), it is possible to calculate the standard free-energy difference between singlets and the $AuPb_3$ phase. The value listed in Table V was calculated from values of Au solubility which were obtained from RT. The standard free-energy differences between the singlets and the N-tuplets and between the singlets and $AuPb_3$ both seem unusually large, considering that the enthalpies of fusion and vaporization of Pb are 1.14 and 46.8 kcal mole^{-1}, respectively, and the associated entropies are 1.90 and 21.2 cal/mole °K.[22] The values given, however, do form a monotonic progression. Further work on this point will be necessary.

VI. DISCUSSION

A. Interstitial defect considerations

The Hägg[23] rule of nonoverlapping atoms for predicting the occurrence of interstitial solutions has undergone several modifications as a result of studies of the fast-diffusing systems. Observation of the interstitial dissolution of noble metals in Pb lead Anthony and Turnbull[24] to require only that ion-core overlap not occur. Na in Pb satisfies this criterion but was found to dissolve substitutionally, suggesting to Owens and Turnbull[25] that a more satisfactory rule would be to require impurity *atoms* to fit into interstices defined by host *ions*. This is the criterion which we shall use in considering possible defect structures for Au in Pb.

Several factors suggest that the doublet and multiplet Au structures may not be substitutional structures. As discussed in Sec. V A, the high Au diffusivity and Au dehancement indicate that simple Au substitutionals do not seem to form in the singlet-doublet equilibrium regime. This implies a relative instability of the substitutionals which presumably arises from the large difference in Pb and Au atomic volumes. Such an inference is supported by density studies on Pb(Au) molten alloys which show the Au to effectively *contract* some 14% in volume.[26,1] This would correspond to a Pb-Au separation of about 3.12 Å, compared to the Goldschmidt separation of 3.19 Å, and suggests the existence of an even greater volume mismatch than follows from a strict hard-sphere estimation. Under these circumstances, if a single substitutional is not particularly stable, then it is hard to see why a disubstitutional or trisubstitutional should be more so. Adding a vacancy to the defect to form an S_2-V or S_3-V should not help, since the effective positive charges on both the Au substitutionals and on the vacancy would repel each other. The difficulty of inducing Au to precipitate[11] from Pb further decreases the likelihood of small ordered clusters of substitutional Pb and Au atoms as defect candidates since such structures should be readily extendible into precipitate particles. Finally, the electron channeling results of Tomlinson and Howie,[27] which were obtained in the region of multiplet stability, appear to be inconsistent with the presence of Au substitutional atoms.

On the other hand, several structures can be conceived which are interstitial in nature and satisfy the same modified Hägg criterion as does the Au-singlet interstitial. Warburton and Turnbull considered two such defects in their discussion of internal-friction effects in the Pb(noble metal) systems.[1,28] These defects were substitutionally sited dimers, and were constituted of two atoms replacing a single host atom and are clearly interstitial defects in the sense which would be measured in a Simmons and Baluffi experiment. It is important to recognize the inherently interstitial nature of these defects while still differentiating them from such structures as di-interstitials, where the impurity atoms actually reside on or near interstitial sites in the structure, as opposed to the substitutionally sited dimers, whose atoms are near substitutional sites.

The Hägg criterion which should pertain in the Pb(Au) system may be deduced by considering the nearest-neighbor (nn) Pb-Au separation of a single Au atom in an octahedral interstice. This value, 2.47 Å, is 0.15 Å greater than the minimum allowed under our criterion, 2.32 Å, which is the sum of the neutral Au and Pb^{+4} radii. Other suggested defects should be tested against these values, and those exceeding the larger may be given particularly serious attention.

Table VI reports the results of such examinations for four substitutionally sited defects: a PbAu dimer, an Au_2 dimer, an Au_3 trimer, and an Au_4 tetramer. In each case the indicated atoms have replaced a single Pb host atom and occupy the resultant cube octahedral void. The defects and surrounding Pb-atom configurations are shown in Fig. 8. The Au atoms are considered to be

TABLE VI. Interatomic distances between Pb and Au atoms for various defect configurations. Since the radius of a Au atom is 1.44 Å (1.37 Å for Au^{+1} ion) and the radius of a Pb^{+4} ion is 0.88 Å, these distances should be compared to the minimal Au-Pb^{+4} separation of 2.32 Å (or 2.25 Å for Au^{+1}-Pb^{+4}).

Number of Au atoms, n	Location	Displacement	nn separation s	ρ_n, number of configurations
1	Octahedral interstice	none	2.47	1
		along ⟨100⟩	$2.47 \leq s \leq 2.68$ [b]	6
2	On lattice site, axis along ⟨100⟩	none	2.68	3
3	On lattice site, in (111) plane	none	2.22	16
	In (100) plane [a]	none	(100) atom: $s = 2.60$, other two: $s = 1.94$	12
		along ⟨100⟩	2.48	
	Off lattice site [b]	arbitrary	$2.22 \leq s \leq 2.51$ [b]	24
4	On lattice site [a]	none	2.30	8
		along ⟨111⟩	2.63 for ⟨111⟩ atom, for others: $s = 2.51$	8

[a] See Fig. 8 for orientation.
[b] See text for comments.

close packed at their metallic radius. When a simple translation of the defect increases the nn Pb-Au separation, that translation and the separations achieved are also listed. The number of defect orientations have been included in Table VI for purposes of entropic calculations.

The nature of these displacements will be obvious from the descriptions in Table VI, with the possible exception of the Au_3 trimer "off lattice site," which refers to configurations of the sort which any three of the four Au_4 tetramer atoms may achieve. In the case of the substitutionally sited PbAu dimer the maximum nn separation has been estimated from the nn separations in the case of the Au_2 dimer. Notice that the Au_4 tetramer ⟨111⟩ displacement was continued until the Pb atoms in the (111) plane and those directly below are equidistant (2.51 Å) from their nn Au atoms.

It is a striking feature of the four defects considered here that each has some configuration whose nn Pb-Au separations are larger than those of the single Au interstitial. Considered in terms of the Hägg criterion, therefore, all should be possible defect structures in the Pb(Au) system. Since confirmation of the existence of such defects would be extremely important to the development of the alloy theory of such systems,[29] we will briefly consider what experimental techniques might differentiate between these proposed interstitial defects and the more traditional substitutional defect structures.

B. Experimental detection of interstitial defects

Internal friction. Results from internal-friction studies of the Pb(noble metal)[13] systems were in fact the stimulus for the original development of the substitutionally sited dimer concept.[1] Although these results have not yet been reproduced,[14,15] the technique should be suitable to the detection of either AuPb or Au_2 dimers, since both should have asymmetric strain fields. The substitutionally sited trimer and tetramer defects are more nearly spherically symmetric and would thus be harder to detect. This is a possible explanation of Sagues and Nowick's failure to observe Au defect peaks,[14] since their temperatures and Au concentrations would have placed them in the range where RT observe diffusion to be multiplet controlled.

Resistivity measurements. If the sensitivity of

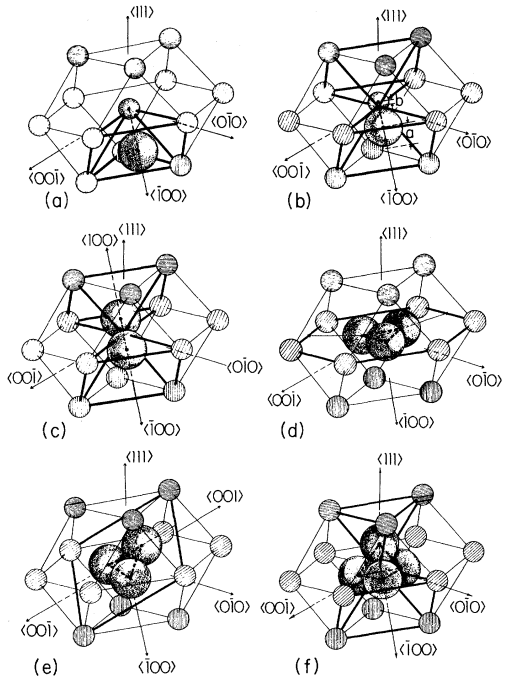

FIG. 8. Various possibilities for Au (large circles) defects in Pb (small circles). Included are (a) conventional interstitial in octahedral interstice, (b) ⟨100⟩ substitutionally sited Au-Pb dimer, (c) ⟨100⟩ substitutionally sited Au-Au dimer, (d) substitutionally sited Au_3 trimer lying in the close-packed (111) plane, (e) substitutionally sited Au_3 trimer lying in the fourfold (100) plane, (f) substitutionally sited Au_4 tetramer arranged as tetrahedron centered in surrounding Pb cube octahedron.

RT's resistivity measurements could be increased, then several possibilities exist. The first would be to try to resolve both the singlet-doublet and singlet-triplet equilibria individually. A second would be to study the kinetics of equilibration in these two reactions. Finally, if Au solubility could be determined accurately at lower temperatures, then some change in energy of dissolution should become evident as doublets and triplets became the stable defects.

Centrifuge measurements. Anthony has shown that the sedimentation profile of a tracer in solid solution depends essentially on the bouyant force on the tracer atoms, which in turn depends on the mass difference between the tracer and the host atoms it replaces.[30] Accordingly, all the substitutionally sited defects should be detectable since a single Pb atom is replaced by 2, 3, or 4 Au atoms respectively. The distinguishability between a classical Au interstitial and either a PbAu or Au_2 dimer would be poor, however, due to the small mass differences involved.

VII. CONCLUSIONS

The diffusivity of Au in Pb(Au) alloys was measured in the dilute-solution limit and a large dehancement effect found. The theory of defect equilibria shows the effect to arise from an equilibrium between fast-diffusing Au singlets and slowly diffusing Au doublets and allows the standard Gibbs free-energy difference g^0_{2-1} between these two defect states to be calculated. This g^0_{2-1} value is incompatible with the value necessary to explain low-temperature Au precipitation behavior from concentrated Pb(Au) alloys, implying the existence of a second equilibrium with an Au multiplet. The configurations of these defects, both doublets and multiplets, are unknown but, considering a modified version of Hägg's rule for the Pb(Au) system, it is considered possible that they belong to a new class of interstitial defects. Several experiments to test this hypothesis are suggested.

ACKNOWLEDGMENTS

I would particularly like to thank Professor D. Turnbull for his suggestions and insights along the course of this work. I also wish to thank Professor A. S. Nowick and Professor T. J. Turner both for helpful discussions along the way and for making their data available to me in advance of publication. The work was supported by the National Science Foundation under Contract No. NSF-GH-40193.

[1]W. K. Warburton and D. Turnbull, in *Diffusion in Solids: Recent Developments*, edited by A. S. Nowick and J. J. Burton (Academic, New York, 1975).
[2]T. R. Anthony, in *Vacancies and Interstitials in Metals*, edited by A. Seeger *et al.* (North-Holland, Amsterdam, 1970).
[3]J. W. Miller, in *Diffusion Processes*, edited by J. N. Sherwood *et al.* (Gordon and Breach, New York, 1971), Vol. 1.
[4]N. L. Peterson, Solid State Phys. 22, 409 (1968).
[5]W. C. Roberts-Austen, Proc. R. Soc. Lond. 59, 281 (1896); 67, 101 (1900).
[6]W. Seith and H. Etzold, Z. Electrochem. 40, 829 (1934).
[7]A. Ascoli, J. Inst. Metals 89, 218 (1960).
[8]G. V. Kidson, Philos. Mag. 13, 247 (1966).
[9]W. K. Warburton, Scr. Metall. 7, 105 (1973).
[10]J. W. Miller, Phys. Rev. B 2, 1624 (1970).
[11]A. N. Rossolimo and D. Turnbull, Acta Metall. 21, 21

(1973).
[12]W. K. Warburton, J. Phys. Chem. Solids 34, 451 (1973).
[13]T. J. Turner, S. Painter, and C. H. Nielsenn, Solid State Commun. 11, 577 (1972).
[14]A. A. Sagues and A. S. Nowick, Solid State Commun. 15, 239 (1974).
[15]T. J. Turner and C. H. Nielsenn, Solid State Commun. 15, 243 (1974).
[16]W. K. Warburton, Phys. Rev. B 7, 1330 (1973).
[17]R. E. Hoffman, D. Turnbull, and E. W. Hart, Acta Metall. 3, 417 (1955).
[18]J. W. Miller, Ph.D. thesis (Harvard University, Cambridge, Mass., 1969) (unpublished).
[19]F. C. Frank and D. Turnbull, Phys. Rev. 104, 617 (1956).
[20]A. J. Leadbetter, D. M. T. Newsham, and N. H. Picton, Philos. Mag. 13, 371 (1966).
[21]R. Feder and A. S. Nowick, Philos. Mag. 15, 805 (1967).
[22]K. A. Gschneidner, Jr., Solid State Phys. 16, 276 (1964).
[23]G. Hägg, Z. Phys. Chem. B 6, 221 (1929); 7, 339 (1930); 8, 445 (1930).
[24]T. R. Anthony and D. Turnbull, Phys. Rev. 151, 495 (1966).
[25]C. W. Owens and D. Turnbull, J. Appl. Phys. 43, 3933 (1972).
[26]A. N. Rossolimo, Ph. D. thesis (Harvard University, Cambridge, Mass., 1971) (unpublished).
[27]P. N. Tomlinson and A. Howie, Phys. Lett. A 27, 491 (1968).
[28]Referred to as "diplons" in Ref. 1 (from Greek *dipl- = twin + -on = particle*. Hence triplon, tetron, etc.), which terminology the author prefers.
[29]D. Turnbull, J. Phys. (Paris) Suppl. 35-C4, 1-10 (1970).
[30]T. R. Anthony, Acta Metall. 18, 877 (1970).